Bioinspiration &
Biomimetics

Running on empty: locomotor compensation preserves fish schooling under hypoxia and informs principles for bioinspired swarms

Bioinspiration & Biomimetics

PAPER

OPEN ACCESS

RECEIVED
29 May 2025

REVISED
15 October 2025

ACCEPTED FOR PUBLICATION
27 October 2025

PUBLISHED
6 November 2025

Running on empty: locomotor compensation preserves fish schooling under hypoxia and informs principles for bioinspired swarms

Yuchen Gong[1], Robert Sterling[2], Xuewei Qi[3], Fidji Berio[1], Otar Akanyeti[2] and Valentina Di Santo[1,*]

[1] Scripps Institution of Oceanography, University of California, San Diego, 9500 Gilman Drive, La Jolla, CA 92093, United States of America
[2] Department of Computer Science, Aberystwyth University, SY23 3DB Aberystwyth, United Kingdom
[3] School of Agriculture, Biomedicine and Environment, La Trobe University, Melbourne, VIC 3086, Australia
* Author to whom any correspondence should be addressed.

E-mail: vdisanto@ucsd.edu

Keywords: schooling fish, collective motion, bioinspired swarm, locomotion, efficiency, hypoxia

Abstract

Environmental stressors such as hypoxia challenge the balance between individual physiological performance and the coordination required for collective behaviors like schooling. Here, we investigate how glass catfish (*Kryptopterus vitreolus*) modulate locomotor and group-level behavior across a gradient of oxygen saturation (95%–20%) while swimming steadily at a constant cruising speed. We found that tailbeat frequency decreased significantly with declining oxygen ($p < 0.0001$), alongside reductions in wave speed ($p = 0.007$). Tailbeat amplitude, by contrast, increased significantly under hypoxia ($p < 0.0001$), and posterior segment angles showed a slight, non-significant increase, consistent with modestly greater tail bending. Despite these changes, the Strouhal number remained fairly constant, and waveform topology was conserved. School structure, including nearest-neighbor distance and distance to the center of the school, remained stable across oxygen treatments, but with significant variation across individual schools. A clear behavioral threshold was observed below 25% oxygen saturation, beyond which coordinated schooling deteriorated. These findings demonstrate that glass catfish employ internally coordinated, energetically economical kinematic adjustments to preserve group cohesion under metabolic constraint. This strategy highlights a decentralized mechanism for sustaining collective behavior near physiological limits and offers biologically-grounded insights relevant to energy-aware coordination in bioinspired swarms.

1. Introduction

Organisms routinely face physiological trade-offs between survival and performance under conditions of resource scarcity, necessitating behavioral and physiological adjustments [1]. Hypoxia, characterized by reduced environmental oxygen availability, is a widespread stressor in aquatic ecosystems that significantly constrains metabolic processes [2, 3]. Although numerous studies have documented individual-level physiological and behavioral responses to hypoxia, including reduced swimming speeds, altered respiratory strategies, and adjustments in behavioral activity [3–6], the collective behavioral responses of fish schools remain relatively understudied, particularly under conditions where swimming speed is experimentally controlled [7].

Schooling behavior provides substantial ecological and energetic advantages to fishes, including enhanced predator avoidance, improved foraging efficiency, and reduced locomotor costs through hydrodynamic interactions [8, 9]. These benefits, however, are generally believed to be contingent on the ability of individuals to maintain precise alignment, stable spacing, and coordinated movement with conspecifics [8], although several studies have

now suggested that a variety of spacing and positioning can confer advantages during schooling [5, 10–15]. Such coordination imposes physiological demands that require continuous sensory processing, rapid decision-making, and sustained muscular activity [16–18]. Under environmental stress, such as hypoxia, the energetic cost of maintaining group cohesion may become unsustainable, potentially disrupting collective behavior. Prior research has demonstrated that hypoxia can influence school structure, often leading to increased inter-individual spacing or reductions in group polarity, thereby weakening the functional benefits of schooling [19, 20]. For instance, schools may expand laterally to improve individual oxygen access, or show reduced maneuverability and turning frequency as fish attempt to conserve energy under metabolic constraint. These changes can increase vulnerability to predators and reduce foraging efficiency, undermining the adaptive value of schooling. However, many of these studies were conducted mostly under 'no-flow' conditions, where fish could adjust their swimming speed or position within the environment in response to oxygen gradients. Without controlling for swimming speed, it is difficult to disentangle whether structural changes in school configuration arise from active behavioral reorganization or passive consequences of reduced activity and motivation. Thus, while previous work has established that hypoxia alters schooling behavior, it remains unclear how these effects unfold when fish are required to sustain a fixed level of locomotor performance—an ecologically relevant scenario for species swimming in flowing water or migratory contexts.

Addressing this critical gap, our study utilizes glass catfish (*Kryptopterus vitreolus*), a small-bodied, obligate schooling species ideal for precise kinematic analyses, to investigate collective responses to hypoxia at a constant cruising speed. By subjecting multiple schools of glass catfish to progressively decreasing oxygen saturation levels while maintaining a constant swimming speed, we were able to explicitly test whether declining oxygen availability triggers structural disruption (manifested as increased spacing and reduced coordination) or elicits subtle, internal compensatory adjustments that enable the preservation of coordinated collective motion. We hypothesized that under progressive hypoxic conditions, schools might either undergo structural fragmentation, indicated by disrupted spacing patterns and diminished coordination, or exhibit compensatory kinematic adjustments that sustain effective schooling despite limited oxygen availability. Furthermore, understanding these adaptive behaviors under metabolic constraints is essential for predicting ecological resilience in natural populations facing environmental degradation and can inform the development of robust, energy-efficient bioinspired robotic swarms. These engineered systems could emulate biological principles to achieve resilient coordination and performance under resource-limited scenarios.

2. Materials and methods

2.1. Animal care and set up

Glass catfish (*Kryptopterus vitreolus*, $n = 35$) were obtained from a licensed wholesale supplier and maintained at approximately 26 °C. The total length and mass of glass catfish were 6.3 ± 0.57 cm and 0.9 ± 0.22 g, respectively (mean ± S.D.). Fish were fed a mix diet of Tetra® flakes and frozen blood worms daily. Each aquarium was independently aerated and filtered, and water quality was maintained through weekly partial water changes. All experimental procedures were conducted under the approved animal care protocol no. 11 924–2020.

2.2. Experimental set-up and schooling kinematics

To decrease oxygen content in the water, we employed a steady oxygen depletion system based on nitrogen displacement [3, 21] (figure 1). Briefly, nitrogen gas was bubbled directly into the swim tunnel to displace dissolved oxygen. The flow of nitrogen was controlled using a nitrogen regulator, a one-way valve, and a gas bubbler, and oxygen concentration in the tank was monitored using a YSI proODO meter. Dissolved oxygen concentration was decreased in a stepwise manner by approximately 5% increments while maintaining a constant temperature of 26 °C. Oxygen levels were progressively reduced from 95% to 20% air saturation, and fish responses were measured at each oxygen level ($n = 16$). At each oxygen concentration, fish were allowed to acclimate for 20 min before schooling behavior was recorded. At the lowest oxygen levels tested, fish were removed and placed in normoxia if they showed any sign of erratic movement or distress.

Schools ($n = 7$) of glass catfish ($n = 5$ fish per school) were filmed ventrally while swimming at $1.3\,\mathrm{BL\,s^{-1}}$ in a Brett-type flow tunnel (Loligo Systems®). The working section was reduced to $23L \times 14W \times 8D$ cm. The swimming speed was selected to represent a typical steady-cruising velocity for small schooling fishes ($1–1.5\,\mathrm{BL\,s^{-1}}$) and to ensure sustained, stable swimming without signs of fatigue or erratic movement. Using a constant, moderate speed allowed us to isolate the effects of oxygen availability on kinematic and schooling variables, minimizing confounding influences of speed-dependent changes in propulsion. High-speed videos were recorded at $500\,\mathrm{frames\,s^{-1}}$ using a Chronos 2.1 camera (Kron Technologies). Videos were taken while fish were swimming in a planar

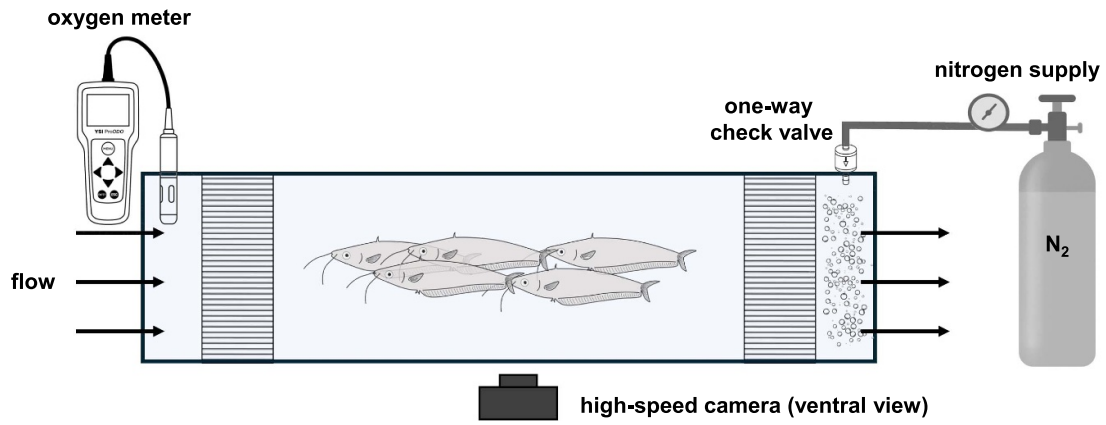

Figure 1. Side-view schematic of the experimental setup: flow tunnel used for glass catfish (*Kryptopterus vitreolus*) schooling experiments under controlled hypoxia. The working section measured $23L \times 14W \times 8D$ cm. Dissolved oxygen level was regulated via a nitrogen supply connected to a one-way valve, and monitored using an oxygen meter. A high-speed camera (ventral view) recorded fish schooling.

(2D) configuration. To ensure consistent 2D recordings, schools were considered planar when all individuals remained within a single horizontal layer, with no evident vertical displacement or overlap. The working section of the flow tunnel (8 cm high) constrained vertical movement relative to the body depth of glass catfish (approximately 1–1.5 cm), promoting naturally planar configurations. This geometry also minimized oxygen gradients within the observation volume, facilitating precise environmental control during hypoxia manipulation. The 2D ventral imaging approach therefore captured the relevant kinematic and spatial parameters for coordinated swimming under controlled flow and oxygen levels (figure 1).

2.3. Kinematics extraction and analysis

To quantify swimming kinematics, we used a custom MATLAB-based tool, CurveMapper, to manually trace the midline of each fish across a sequence of frames from high-speed video [22, 23]. The digitized midlines were first rotated and translated so that the fish's anterior-posterior axis aligned with the x-axis (from right to left) in our coordinate system (figure 2(a)) [22]. Rotation was performed using the mean body orientation angle, calculated as the average of the orientation angles of all midlines. To determine the orientation angle of each midline, a linear regression line was fitted to its coordinates, and the orientation was obtained from the slope of the fitted line. After rotation, translation along the y-axis was applied by detrending each midline, with the linear trend computed from the tail tip displacement. Next, the tail-beat amplitude (A) and frequency (f) were calculated by fitting a sine wave to the tail-tip displacement across frames using a least-squares method,

$$y = A\sin(wt + \phi) \tag{1}$$

where t is the time stamp, $w = 2\pi f$ is the angular frequency, and ϕ is the phase angle. The Strouhal number (non-dimensional number measuring hydrodynamic efficiency) was derived from tail beat amplitude, frequency and swimming speed (U),

$$St = \frac{2Af}{U}. \tag{2}$$

To estimate the body wavespeed (V), we extended the sine wave fitting to two additional midline points (50% and 75% down the body). The phase difference between three sine models (i.e. 50%, 75% and tail tip) indicated the time required for the wave to travel from the mid part of the body to the tail tip (figure 2(b)). The wavelength (λ) was derived from wavespeed and tail beat frequency,

$$\lambda = \frac{V}{f} \tag{3}$$

and, finally the slip ratio (non-dimensional number measuring swimming efficiency) was calculated as the ratio between swimming speed (U) and body wavespeed (s is typically less than one, and it is assumed that swimming efficiency increases as s gets closer to 1),

$$s = \frac{U}{V}. \tag{4}$$

To quantify spatial organization within fish schools, several parameters were computed for each individual fish within the school. The nearest-neighbor distance (NND) represents the shortest distance between each fish and its nearest neighbor.

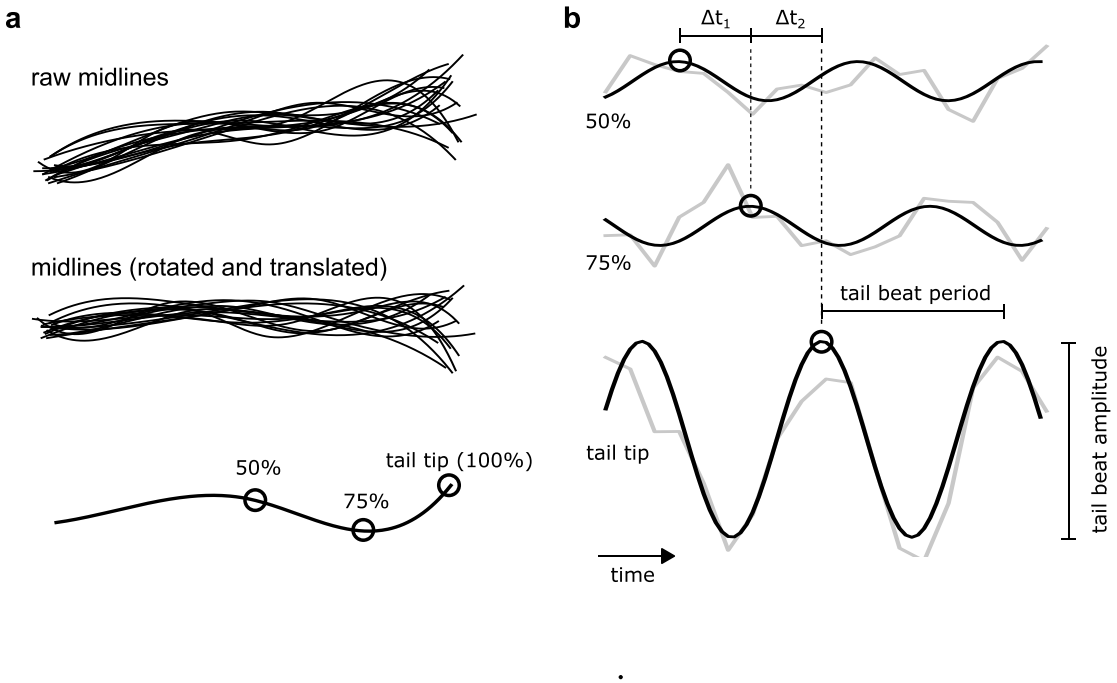

Figure 2. Kinematics analysis: tail beat amplitude, tail beat frequency and body wavespeed calculation. (a) Raw and preprocessed midlines (rotated and translated). (b) Time-varying body amplitude (gray) and fitted sine model (black) for three positions along the body: 50% (top), 75% (middle) and tail tip (bottom). These three positions are shown in (a) (bottom). Tail beat amplitude and frequency were extracted from the tail tip sine model. Body wavespeed was calculated from the phase difference between the three sine models.

Distance to the center (DC) was calculated as the mean pairwise distance among the five fish, representing their proximity to the group centroid. Furthermore, the mean distance (MD) represents the average pairwise distance between a focal fish and all other individuals in the group, providing an overall measure of spatial dispersion. These metrics offer insight into local and global spacing patterns within the school. In addition to spatial structure metrics, we quantified the total distance traveled by each fish within the school as an indicator of positional stability [18]. The trajectory of the snout was tracked across frames, and displacement—regardless of direction—was standardized to one-second intervals ($BL\,s^{-1}$) to account for differences in fin beat duration. This metric captures overall positional adjustments made by individuals within the school during steady swimming and was used to assess how oxygen availability influenced school dynamics and positional stability among group members.

2.4. Body segment analysis

Further kinematic analysis was performed by translating continuous fish midlines into discrete multi-segment models using the segment growing algorithm described in [24]. These models, which describe fish midlines as a series of rigid segments connected by joints, can be used to compare swimming kinematics across species and treatments, and may help design fish-inspired robots. Starting from the snout, the segment growing algorithm performed a linear search for optimal joint placements to create the longest possible segments while keeping the model error below a user-defined threshold. During model estimation, the error calculations were based on the area between the linear segment and the fish midline (i.e. the larger the area, the bigger the error), and the error threshold was set to $0.05\,L^2$ (determined after preliminary investigations of several fish midline sets). In addition, during model estimation, the minimum segment length was set to $0.1\,L$ to ensure that the segment creation process was not overly sensitive to midline digitization noise and large tail amplitudes.

Multi-segment models provide valuable insights into how midline kinematics varied with oxygen saturation. The model size (i.e. number of joints) is positively correlated with the amount of bending. Midlines with higher curvatures would typically require larger models (i.e. more segments/joints). Similarly, the distribution of the joints throughout the body is linked to body wavelength and amplitude envelope. To quantify joint distributions, we calculated the covariance of the lengths and positions of the segments. A negative covariance would indicate a higher joint density toward the tail (typically seen

in fishes [25]), whereas zero covariance would suggest evenly spaced joints along the body (i.e. segments with equal lengths). The length of the first segment (hereafter head segment) would be indicative of the point of initiation of the undulatory wave, and the length of the last segment (hereafter tail segment) is expected to be shorter than that of the head segment (if covariance is negative). In addition, we investigated how the angle of the segments (with respect to the direction of swimming) varied along the body.

2.5. Statistical analyses

For each school and oxygen level, measurements from individual fish were averaged, yielding one data point per school per oxygen treatment. Analyses of swimming kinematics and inter-individual distances in relation to oxygen saturation levels were conducted using repeated-measures ANOVA, with oxygen as a fixed factor and school ID as a random factor. All statistical tests were performed with a significance threshold of $\alpha = 0.05$ in JMP Pro, version 18 (SAS Institute Inc.).

3. Results

Glass catfish maintained a consistent cruising swimming speed of 1.3 BLs^{-1} across all oxygen concentrations, indicating a strong maintenance of group-level locomotor performance under varying environmental conditions. However, individual-level kinematic variables were significantly influenced by oxygen levels especially below 60% saturation (table 1). Tailbeat amplitude increased significantly with declining oxygen ($F = 51.2,\ p < 0.0001$), differed among schools ($F = 13.7,\ p < 0.0001$), and showed a significant *oxygen* × *school* interaction ($F = 4.5,\ p = 0.0004$), suggesting that individuals modulate tail displacement in response to hypoxia in a school-specific manner (figure 3(a)). In contrast, tailbeat frequency decreased significantly as oxygen declined ($F = 62.1,\ p < 0.0001$), also exhibiting significant effects of school ($F = 19.9,\ p < 0.0001$) and an *oxygen* × *school* interaction ($F = 4.2,\ p = 0.0007$, figure 3(b)). Strouhal number (St) was not significantly affected by oxygen levels ($p = 0.3$) but varied among schools ($F = 11.0,\ p < 0.0001$), indicating stable propulsive efficiency across environmental conditions, yet differences in swimming dynamics among school groups (figure 3(c)). Wavelength also remained constant with respect to oxygen ($p = 0.5$) but differed among schools ($F = 2.4,\ p = 0.03$), further supporting baseline variation in kinematic patterns between groups (figure 3(d)).

In contrast, wave speed declined significantly under hypoxia ($F = 7.5, p = 0.007$, figure 3(e)), while slip ratio approached 1 with decreasing oxygen ($F = 18.1,\ p < 0.0001$) suggesting increased locomotor efficiency with progressive hypoxia. We found a significant *oxygen* × *school* interactive effect on slip ($F = 3.1,\ p = 0.01$, figure 3(f)). This may reflect compensatory kinematic adjustments that maintain swimming speed while reducing the cost of transport.

Despite changes in locomotor parameters, group structure remained stable across oxygen treatments (figure 4). Distance to the center of the school was not significantly affected by oxygen ($p = 0.9$, figure 4(a)), though it differed strongly across schools ($F = 8.1,\ p < 0.0001$, figure 4(b)). Similarly, NND was unaffected by oxygen levels ($F = 1.5,\ p = 0.2$, figure 4(c)), but differed significantly between schools ($F = 4.6,\ p = 0.0004$, figure 4(d)). MD across fish in the school was also not affected by oxygen levels ($p = 0.5$) but differed with schools ($F = 7.3,\ p < 0.0001$). These results highlight group-specific spacing behaviors that are resilient to oxygen-induced disruption. At 25% oxygen saturation, a subset of individuals ceased swimming, and at 20%, the majority became inactive. This suggests a hypoxia threshold below which sustained locomotion and coordinated schooling can no longer be maintained at 1.3 $BL\,s^{-1}$. We found a significant effect of oxygen on the stability of the school, measured as the distance traveled by fish in a school, standardized for one second. We found that with higher oxygen levels associated with greater distance traveled per second ($F = 13.4,\ p = 0.0004$, figure 4(e). We also found significant baseline differences in swimming speed among schools ($F = 33.1,\ p < 0.0001$, figure 4(f). Together, these results show that fish are less likely to shift their position within the group with decreasing oxygen availability, and that this relationship is consistent across schools.

Multi-segment models Figure 5(a) shows raw midlines and its multi-segment model for one representative fish. The majority of the models had negative covariance suggesting that joints were more densely packed at the posterior body (mean±std: −316.3±24.8). This pattern did not vary with O_2 level ($p < 0.6$) (figure 5(b)). To further investigate the effect of oxygen saturation, models were divided into three groups: low O_2 ($\leqslant 30\%$), medium O_2 ($> 30\%$ and $< 90\%$) and high O_2 ($\geqslant 90\%$). In all three groups, more than 50% of the models had six joints (i.e. seven segments): 68% in low O_2, 58% in medium O_2 and 54% in high O_2 (figure 5(c)). Further analysis on these models showed that the segments got progressively shorter toward the tail corroborating covariance results (figures 5(d) and (e)). The length ratio between head and tail segments was 2.2. Finally, the angle of segments increased exponentially toward the tail (figure 5(f)). The angle ratio between head and tail segments was 0.21. There was no significant difference in joint positions, segment lengths and angles

Table 1. Swimming kinematics and group structure metrics (means ± S.E.) for schools of glass catfish *Kryptopterus vitreolus* ($n = 7$ schools, $n = 5$ fish each school). A = tail amplitude, TBF = tail beat frequency, BL = body lengths.

O_2%	*A* (BL)	TBF (Hz)	Wavelength (BL)	Wave speed (BL s^{-1})	Slip ratio
95	0.05 ± 0.00	5.51 ± 0.34	0.53 ± 0.06	2.91 ± 0.26	0.60 ± 0.05
90	0.04 ± 0.00	5.87 ± 0.42	0.91 ± 0.17	5.43 ± 1.36	0.47 ± 0.05
85	0.05 ± 0.01	6.32 ± 0.30	0.89 ± 0.15	5.95 ± 1.47	0.41 ± 0.03
80	0.05 ± 0.01	5.88 ± 0.43	0.66 ± 0.09	3.78 ± 0.49	0.50 ± 0.05
75	0.05 ± 0.01	5.75 ± 0.33	1.05 ± 0.17	6.11 ± 1.01	0.41 ± 0.04
70	0.05 ± 0.01	5.68 ± 0.25	0.59 ± 0.07	3.35 ± 0.43	0.52 ± 0.03
65	0.05 ± 0.01	5.41 ± 0.26	0.60 ± 0.10	3.15 ± 0.54	0.56 ± 0.04
60	0.04 ± 0.01	5.86 ± 0.58	0.52 ± 0.10	2.92 ± 0.47	0.58 ± 0.06
55	0.06 ± 0.00	5.00 ± 0.29	0.64 ± 0.09	3.14 ± 0.41	0.58 ± 0.04
50	0.06 ± 0.00	5.30 ± 0.31	0.78 ± 0.12	4.31 ± 0.88	0.55 ± 0.06
45	0.06 ± 0.01	5.06 ± 0.27	0.67 ± 0.10	3.56 ± 0.83	0.60 ± 0.04
40	0.06 ± 0.00	4.87 ± 0.29	0.64 ± 0.07	3.05 ± 0.33	0.59 ± 0.04
35	0.07 ± 0.01	4.52 ± 0.42	0.61 ± 0.06	2.72 ± 0.24	0.68 ± 0.05
30	0.06 ± 0.00	4.53 ± 0.35	0.73 ± 0.11	3.17 ± 0.45	0.59 ± 0.09
25	0.07 ± 0.00	4.38 ± 0.18	0.73 ± 0.11	3.28 ± 0.59	0.62 ± 0.09
20	0.07 ± 0.00	4.38 ± 0.11	0.73 ± 0.16	3.22 ± 0.70	0.67 ± 0.08

across three O_2 groups. Nevertheless, we noticed that in segment angles plot (figure 5(f)) there was a visible separation between three groups after segment four, i.e. low O_2 having slightly bigger angles than high O_2 group and medium O_2 group falling in between. These minute differences in segment angles would explain the higher tail beat amplitudes observed at low oxygen saturation levels (figure 3(a)).

4. Discussion

Glass catfish exhibited clear locomotor modulation under hypoxia, with reduced tailbeat frequency and wave speed but increased amplitude. Despite these adjustments, fish maintained a constant swimming speed of 1.3 BL s^{-1} and preserved school cohesion across a wide range of oxygen concentrations. These compensations contrast with many other species, where hypoxia often causes schools to spread or fragment [4, 19]. Our results show that internal kinematic adjustments—rather than spatial reorganization—enable collective behavior to persist under moderate oxygen stress.

The significant decline in tailbeat frequency under hypoxia, coupled with increased tailbeat amplitude, suggests a strategic reorganization of propulsion. Increased amplitude under reduced oxygen conditions likely reflects recruitment of anaerobic white muscle fibers, which generate greater contractile forces, enabling larger body undulations which are typically seen during unsteady swimming such as forward accelerations [26–29]. This muscular shift may allow fish to sustain thrust output despite reduced aerobic metabolic capacity. Contrary to our initial expectation, the reduction in tailbeat frequency highlights a flexible temporal strategy rather than a fixed timing of locomotor cycles. Nevertheless, collective swimming persisted despite frequency shifts [5].

Importantly, the Strouhal number remained within the same range of across treatments, indicating that amplitude and frequency changes were modulated to maintain propulsive efficiency. The coordinated changes of tailbeat amplitude and frequency observed here is consistent with a documented control strategy in fishes to maintain propulsive efficiency under varying environmental or flow conditions. For example, Liao *et al* [30] showed that trout swimming in a vortex street adjust both amplitude and frequency simultaneously to remain synchronized with the vortex shedding frequency. Similarly, Akanyeti and Liao [31] found that rainbow trout modulate tailbeat amplitude and frequency in opposite directions as flow speed increases, maintaining a nearly constant Strouhal number and stable wake structure. Comparable coordinated kinematic adjustments have been reported in other fishes [32, 33]. Together, these studies suggest that simultaneous tuning of amplitude and frequency represents a robust locomotor control mechanism—one that, in this case, enables glass catfish to preserve hydrodynamic efficiency under hypoxia. Thus, fish optimized their locomotor mechanics to preserve mechanical efficacy and minimize energy expenditure without reducing swimming speed. Such modulation of body undulations and pressure gradients around the body may also enhance respiratory efficiency, a critical adjustment during hypoxia [34].

Multi-segment modeling showed consistent undulatory patterns across oxygen levels, with stable joint positions and segment lengths. However, posterior segment angles increased slightly under hypoxia, particularly in segments closer to the tail. These

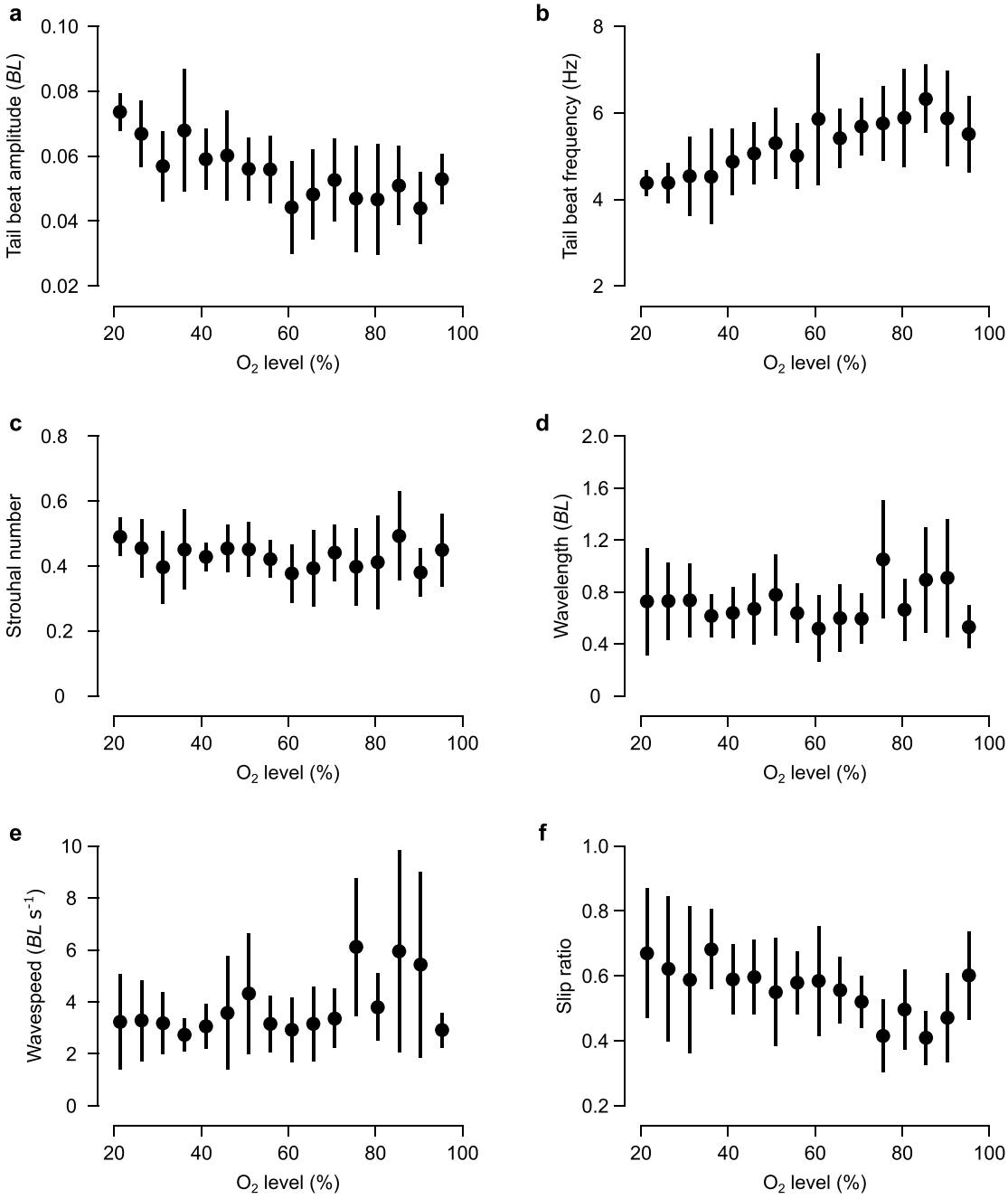

Figure 3. Kinematics results of schooling fish under varying oxygen saturation levels. (a) Tail beat amplitude. (b) Tail beat frequency. (c) Strouhal number. (d) Wavelength. (e) Wavespeed. (f) Slip ratio. In all plots, each data point and error bar show mean ± standard deviation across all seven experimental groups.

subtle shifts likely underlie the observed amplitude increases, revealing how fish modulate their kinematic output within a conserved neuromechanical framework to sustain propulsion under metabolic constraint.

Group structure remained stable, with no significant change in spacing until oxygen levels dropped below 25%. This persistence highlights the resilience of decentralized interactions under physiological stress. Increased positional stability at low oxygen suggests reduced overall movement—an energy-saving strategy that minimizes unnecessary repositioning while preserving alignment [18]. Coordinated swimming is generally thought to lower, not raise, individual energetic cost: hydrodynamic interactions among neighbors reduce drag and muscle activity [8, 10, 35]. Glass catfish maintained schooling under hypoxia by tuning tailbeat kinematics to sustain hydrodynamic efficiency and cohesion, indicating that the benefits of schooling outweigh its potential costs even under metabolic constraint.

Significant variability in kinematics and spacing among different schools indicates that local environmental history or individual physiological thresholds may shape collective responses. Although

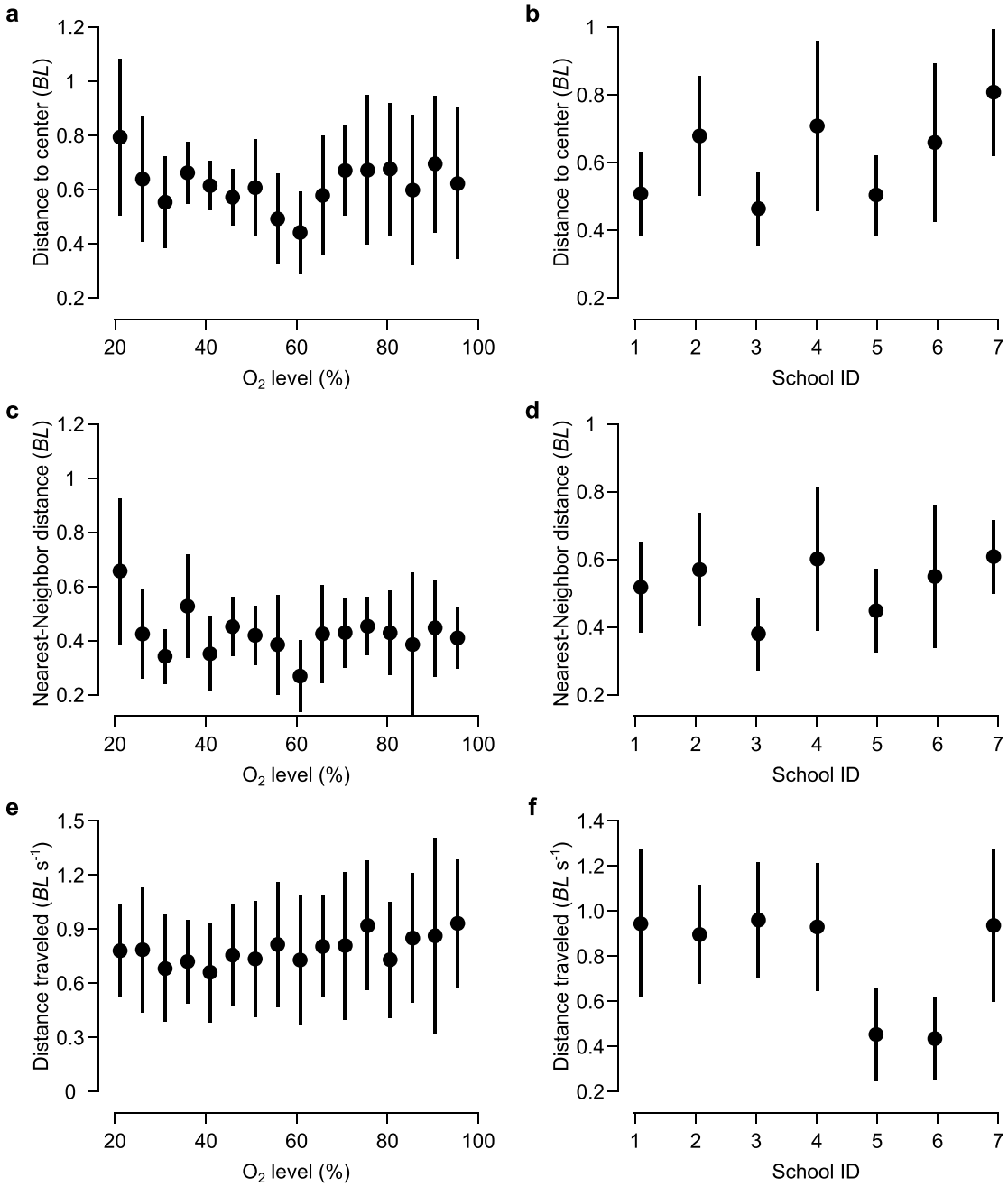

Figure 4. Comparison of group dynamics under varying oxygen saturation levels and among schools. (a) and (b) Distance to the center. (c) and (d) Nearest-neighbor distance. (d) and (e) Distance traveled (per second). In all plots, each data point and error bar show mean ± standard deviation across all seven experimental groups.

all individuals within schools were familiar with one another, groups could develop distinct collective personalities, differing in baseline cohesion, alignment, or responses to flow. These group-level signatures emerge from social interactions which align with theoretical models of distributed decision-making, where group coordination emerges from locally adaptive yet heterogeneous responses [36]. The sharp behavioral threshold at approximately 25% oxygen saturation marks the physiological limit at which internal compensatory mechanisms fail, resulting in a decline in coordinated schooling. Understanding such thresholds has crucial ecological implications for assessing the resilience of fish populations to environmental stressors such as climate-driven hypoxia [37]. While our ventral imaging approach captured all relevant kinematic and spacing parameters within the planar school, future studies incorporating 3D tracking will be valuable to explore potential vertical components of collective motion under hypoxia in this and other species.

Our findings contrast with previous studies showing that hypoxia often disrupts schooling through increased spacing, reduced maneuverability, or complete disbandment. In species such as Atlantic herring, progressive hypoxia in still-water leads to

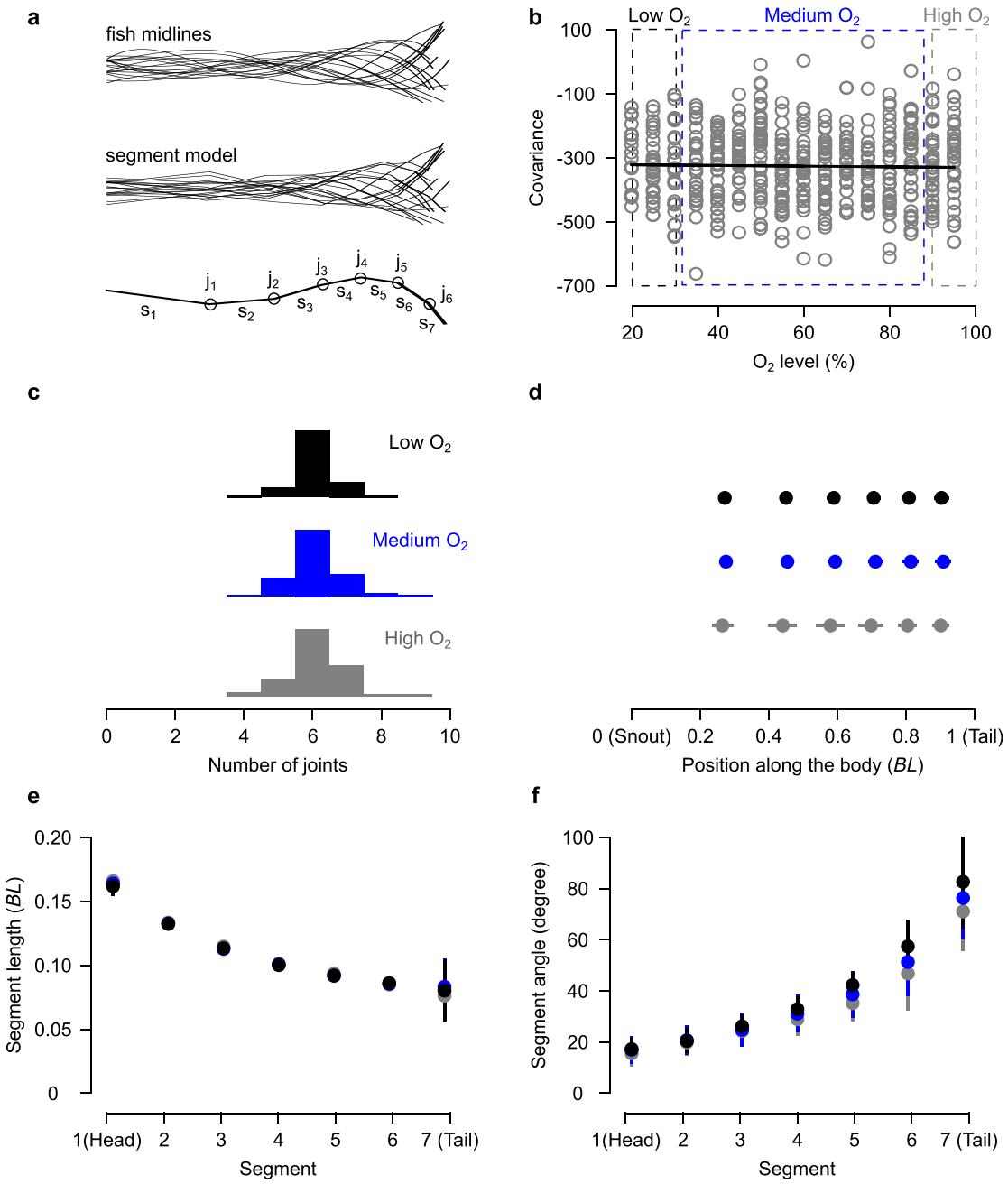

Figure 5. Multi-segment models. (a) Raw midlines and its multi-segment model for one representative fish. The data was captured while fish was swimming at 1.3 BL s^{-1} at 90% O_2 level (school id: 1, fish id: 1). Segments and joints are shown for one midline (bottom). (b) Covariance between joint positions and segment lengths across different O_2 levels. Data from all models (gray circles) and the regression line (black line) were plotted. Models were grouped into three categories for further analysis, low O_2, medium O_2 and high O_2. (c) Histogram (count) of number of joints. Median (six-joint models) was chosen for further comparison between three O_2 levels: (d) Joint positions along the body; (e) segment lengths; and (f) segment angles (peak to peak). In (d)–(f), mean values (filled circular markers) were not significantly different between three O_2 levels. Error bars show the standard deviation from the mean.

transient increases in swimming speed followed by the breakdown of school structure below 30% oxygen saturation [38]. Other species maintain school integrity but reduce activity levels and turning rates, presumably to conserve energy under declining oxygen conditions [39]. These behavioral changes have been interpreted as strategies to balance group cohesion with physiological stress. In contrast, glass catfish in our study exhibited no significant change in inter-individual spacing or school geometry across oxygen treatments. This divergence may stem from a critical methodological difference: whereas previous studies were conducted in still water where fish could freely modulate their swimming speed, our experiments imposed a constant flow speed. As a result, fish were required to maintain position in the flow or drop out of the school entirely. Under this constraint, individuals did not reorganize spatially, but instead compensated internally—reducing tailbeat frequency and wave speed while increasing amplitude—to sustain

thrust and preserve synchronization. These results suggest that environmental context fundamentally shapes how fish balance energetic limitations with collective demands. When swimming speed is non-negotiable, internal kinematic plasticity may offer a more viable route to maintaining group cohesion than spatial reorganization.

Fish locomotion is an energetically demanding process that relies on precise coordination between muscle activity, oxygen transport, and metabolic regulation. Under normoxic conditions, sustained swimming is primarily powered by aerobic red muscle, which supports efficient, low-intensity movement. However, as oxygen availability declines, the capacity for aerobic ATP production diminishes, forcing fish to increasingly rely on anaerobic white muscle fibers to maintain propulsion [40]. This shift often results in reduced endurance and altered kinematics, such as increased tailbeat amplitude and reduced frequency, reflecting compensatory strategies to sustain thrust output with lower aerobic efficacy. Individual variation in hypoxia tolerance further shapes locomotor capacity: fish with higher aerobic scope or more efficient oxygen uptake tend to maintain better swimming performance under low oxygen, while others exhibit early onset of fatigue or behavioral suppression [41]. In some species, hypoxia elicits a metabolic depression—a downregulation of total energy expenditure—which may include reduced muscle excitability or recruitment, further constraining locomotor ability [42]. These physiological responses can directly influence movement patterns, such as reduced activity, loss of coordination, or complete cessation of swimming at critically low oxygen thresholds [3]. In our study, the maintenance of swimming speed under hypoxia required internal kinematic adjustments rather than reduced activity, indicating that fish modulated their muscular effort—likely through altered recruitment patterns—to preserve locomotor output despite declining aerobic capacity. These findings highlight the interplay between oxygen availability, muscle physiology, and locomotor performance in shaping how fish cope with environmental stress.

The compensatory strategies of glass catfish offer a useful model for bioinspired robotics. Their ability to sustain coordinated motion under energetic constraint—by increasing amplitude while preserving synchrony—illustrates a local control strategy that decouples power output from coordination. In robotic swarms, similar rules could allow individual units to modulate actuation under limited energy or resistance without breaking formation, conserving power while maintaining collective function. Variation among schools further highlights the value of decentralized adaptation: cohesion persisted despite differences in individual kinematics. Analogously, robotic agents need not behave identically to remain coordinated; allowing local adjustments based on internal state, such as battery level or sensor feedback, could enhance resilience in resource-limited environments. Such biologically inspired strategies demonstrate how internal modulation can sustain group performance even when energy availability fluctuates.

5. Conclusions

This study shows that glass catfish sustain coordinated group behavior under hypoxic stress through finely tuned kinematic modulation rather than structural reorganization. Individuals adjusted tailbeat frequency and amplitude simultaneously to preserve swimming speed and cohesion as oxygen declined. The conserved Strouhal number and waveform topology across treatments indicate that propulsion remained mechanically efficient despite metabolic constraint. School geometry also remained stable, and the emergence of school-specific kinematic strategies suggests that group resilience arises from decentralized, locally adaptive responses. Multi-segment modeling supports this view, revealing conserved body structure but slightly increased posterior angles under hypoxia, likely driving the observed amplitude rise. A clear behavioral threshold occurred near 25% oxygen saturation, below which coordination declined—marking the physiological limit of compensation and the boundary between adaptation and collapse. Together, these results identify a robust mechanism of locomotor compensation that preserves schooling under oxygen stress and provide a quantitative framework for distributed adaptation in collective systems, with implications for energy-aware coordination in bioinspired multi-agent platforms.

Data availability statement

All data that support the findings of this study are available in a public GitHub repository at: https://github.com/vdisanto/glasscatfishschooling-hypoxia.git.

Acknowledgements

This work was funded by an early career grant from the Swedish Research Council (Award No. 2021-04400) and start-up funds at UC San Diego to Valentina Di Santo, and by the European Commission to Otar Akanyeti (H2020-MSCA-RISE-2019, Grant Number: 873178). We thank members of the Di Santo Lab for the care of the fish used in this study.

Conflict of interest

The authors declare no conflict of interest.

Author contributions

Yuchen Gong 0000-0002-4614-9164
Data curation (equal), Formal analysis (equal), Project administration (equal), Visualization (equal), Writing – original draft (equal)

Robert Sterling 0009-0005-0605-8195
Formal analysis (equal), Investigation (equal), Validation (equal), Visualization (equal), Writing – review & editing (equal)

Xuewei Qi 0000-0002-6146-9668
Formal analysis (equal), Investigation (equal), Methodology (equal), Writing – review & editing (equal)

Fidji Berio 0000-0003-0810-9783
Investigation (equal), Writing – review & editing (equal)

Otar Akanyeti 0000-0003-3515-6833
Data curation (equal), Formal analysis (equal), Funding acquisition (lead), Investigation (equal), Validation (equal), Visualization (equal), Writing – review & editing (equal)

Valentina Di Santo 0000-0002-5419-3747
Conceptualization (lead), Data curation (equal), Formal analysis (equal), Funding acquisition (lead), Investigation (equal), Methodology (equal), Project administration (equal), Resources (lead), Supervision (lead), Writing – original draft (equal), Writing – review & editing (equal)

References

[1] Altieri A H and Gedan K B 2015 Climate change and dead zones *Glob. Change Biol.* **21** 1395–406
[2] Richards J G 2009 Metabolic and molecular responses of fish to hypoxia *Fish Physiol.* **27** 443–85
[3] Di Santo V, Tran A H and Svendsen J C 2016 Progressive hypoxia decouples activity and aerobic performance of skate embryos *Conserv. Physiol.* **4** cov067
[4] Herbert N A and Steffensen J F 2006 Hypoxia increases the behavioural activity of schooling herring: a response to physiological stress or respiratory distress? *Mar. Biol.* **149** 1217–25
[5] Killen S S, Marras S, Ryan M R, Domenici P and McKenzie D J 2012 A relationship between metabolic rate and risk-taking behaviour is revealed during hypoxia in juvenile european sea bass *Funct. Ecol.* **26** 134–43
[6] Lubitz N *et al* 2024 Climate change-driven cooling can kill marine megafauna at their distributional limits *Nat. Clim. Change* **14** 526–35
[7] Di Santo V 2022 Ecophysiomechanics: integrating energetics and biomechanics to understand fish locomotion under climate change *Integr. Comparative Biol.* **62** 711–20
[8] Weihs D 1973 Hydromechanics of fish schooling *Nature* **241** 290–1
[9] Shaw E 1978 Schooling fishes: the school, a truly egalitarian form of organization in which all members of the group are alike in influence, offers substantial benefits to its participants *Am. Sci.* **66** 166–75
[10] Ashraf I, Bradshaw H, Ha T-T, Halloy J, Godoy-Diana R and Thiria B 2017 Simple phalanx pattern leads to energy saving in cohesive fish schooling *Proc. Natl Acad. Sci.* **114** 9599–604
[11] Hemelrijk C K, Reid D, Hildenbrandt H and Padding J 2015 The increased efficiency of fish swimming in a school *Fish Fish.* **16** 511–21
[12] Marras S, Killen S S, Lindström J, McKenzie D J, Steffensen J F and Domenici P 2015 Fish swimming in schools save energy regardless of their spatial position *Behav. Ecol. Sociobiol.* **69** 219–26
[13] Pan Y and Lauder G V 2024 Combining computational fluid dynamics and experimental data to understand fish schooling behavior *Integr. Comparative Biol.* **64** 753–68
[14] Thandiackal R and Lauder G 2023 In-line swimming dynamics revealed by fish interacting with a robotic mechanism *eLife* **12** e81392
[15] Zhang Y and Lauder G V 2025 Physics and physiology of fish collective movement *Newton* **1** 100021
[16] Peterson A N, Swanson N and McHenry M J 2024 Fish communicate with water flow to enhance a school's social network *J. Exp. Biol.* **227** jeb247507
[17] McKee A, Soto A P, Chen P and McHenry M J 2020 The sensory basis of schooling by intermittent swimming in the rummy-nose tetra (hemigrammus rhodostomus) *Proc. R. Soc. B* **287** 20200568
[18] Berio F, Morerod C, Qi X and Di Santo V 2023 Ontogenetic plasticity in shoaling behavior in a forage fish under warming *Integr. Comp. Biol.* **63** 730–41
[19] Moss S and McFarland W 1970 The influence of dissolved oxygen and carbon dioxide on fish schooling behavior *Mar. Biol.* **5** 100–7
[20] Domenici P, Steffensen J F and Marras S 2017 The effect of hypoxia on fish schooling *Phil. Trans. R. Soc. B* **372** 20160236
[21] Bennett W A and Beitinger T L 1995 Technical notes: Overview of techniques for removing oxygen from water and a description of a new oxygen depletion system *North Am. J. Aquacult.* **57** 84–87
[22] Di Santo V, Goerig E, Wainwright D K, Akanyeti O, Liao J C, Castro-Santos T and Lauder G V 2021 Convergence of undulatory swimming kinematics across a diversity of fishes *PNAS* **118** e2113206118
[23] Goerig E, Di Santo V, Wainwright D K, Castro-Santos T, Liao J, Akanyeti O and Lauder G 2021 Convergence of undulatory swimming kinematics across a diversity of fishes *Zenodo* (https://doi.org/10.5281/zenodo.4623882)
[24] Fetherstonhaugh S E, Shen Q and Akanyeti O 2021 Automatic segmentation of fish midlines for optimizing robot design *Bioinspir. Biomim.* **16** 046005
[25] Akanyeti O, Di Santo V, Goerig E, Wainwright D K, Liao J C, Castro-Santos T and Lauder G V 2022 Fish-inspired segment models for undulatory steady swimming *Bioinspir. Biomim.* **17** 046007
[26] Akanyeti O, Ortega J, Yanagitsuru Y R, Lauder G V, Stewart W J and Liao J C 2017 Accelerating fishes increase propulsive efficiency by modulating vortex ring geometry *Proc. Natl Acad. Sci.* **114** 13828–33
[27] Wen L, Ren Z, Di Santo V, Hu K, Yuan T, Wang T and Lauder G V 2018 Understanding fish linear acceleration using an undulatory biorobotic model with soft fluidic elastomer actuated morphing median fins *Soft Robot.* **5** 375–88
[28] Altringham J D and Ellerby D J 1999 Fish swimming: patterns in muscle function *J. Exp. Biol.* **202** 3397–403
[29] Jayne B and Lauder G 1994 How swimming fish use slow and fast muscle fibers: implications for models of vertebrate muscle recruitment *J. Comparative Physiol. A* **175** 123–31
[30] Liao J C, Beal D N, Lauder G V and Triantafyllou M S 2003 Fish exploiting vortices decrease muscle activity *Science* **302** 1566–9
[31] Akanyeti O and Liao J C 2013 A kinematic model of kármán gaiting in rainbow trout *J. Exp. Biol.* **216** 4666–77
[32] Tytell E D and Lauder G V 2004 The hydrodynamics of eel swimming: I. Wake structure *J. Exp. Biol.* **207** 1825–41

[33] Saadat M, Fish F E, Domel A, Di Santo V, Lauder G and Haj-Hariri H 2017 On the rules for aquatic locomotion *Phys. Rev. Fluids* **2** 083102
[34] Akanyeti O, Thornycroft P J, Lauder G V, Yanagitsuru Y R, Peterson A N and Liao J C 2016 Fish optimize sensing and respiration during undulatory swimming *Nat. Commun.* **7** 11044
[35] Di Santo V 2024 Schooling in fishes *Encyclopedia of Fish Physiology* vol 2, 2nd edn (Academic) pp 614–25
[36] Couzin I D *et al* 2003 Self-organization and collective behavior in vertebrates *Adv. Study Behav.* **32** 10–1016
[37] Di Santo V and Goerig E 2025 Swimming smarter, not harder: fishes exploit habitat heterogeneity to increase locomotor performance *J. Exp. Biol.* **228** JEB247918
[38] Domenici P, Steffensen J F and Batty R S 2000 The effect of progressive hypoxia on swimming activity and schooling in atlantic herring *J. Fish Biol.* **57** 1526–38
[39] Domenici P, Herbert N, Lefrançois C, Steffensen J and McKenzie D 2013 The effect of hypoxia on fish swimming performance and behaviour *Swimming Physiology of Fish: Towards Using Exercise to Farm a Fit Fish in Sustainable Aquaculture* (Springer) 129–59
[40] Dwyer G K, Stoffels R J and Pridmore P A 2014 Morphology, metabolism and behaviour: responses of three fishes with different lifestyles to acute hypoxia *Freshwater biol.* **59** 819–31
[41] Pang X, Pu D-Y, Xia D-Y, Liu X-H, Ding S-H, Li Y and Fu S-J 2021 Individual variation in metabolic rate, locomotion capacity and hypoxia tolerance and their relationships in juveniles of three freshwater fish species *J. Comp. Physiol. B* **191** 755–64
[42] Rossi G S and Wright P A 2020 Hypoxia-seeking behavior, metabolic depression and skeletal muscle function in an amphibious fish out of water *J. Exp. Biol.* **223** jeb213355